doi:10.1093/jmcb/mjz115
Published online January 3, 2020

Article

Dependence of sperm structural and functional integrity on testicular calcineurin isoform PPP3R2 expression

Yue Liu[1], Chujun Zhang[2], Shiyao Wang[2], Yanqin Hu[1], Jia Jing[1], Luyao Ye[2], Ran Jing[2], and Zhide Ding[1,*]

[1] Department of Histology, Embryology, Genetics and Developmental Biology, Shanghai Key Laboratory for Reproductive Medicine, Shanghai Jiao Tong University School of Medicine, Shanghai 200025, China
[2] Department of Clinical Medicine, Shanghai Jiao Tong University School of Medicine, Shanghai 200025, China
* Correspondence to: Zhide Ding, E-mail: zding@shsmu.edu.cn

Edited by Jinsong Li

After leaving the testis, mammalian sperm undergo a sequential maturation process in the epididymis followed by capacitation during their movement through the female reproductive tract. These phenotypic changes are associated with modification of protein phosphorylation and membrane remodeling, which is requisite for sperm to acquire forward motility and induce fertilization. However, the molecular mechanisms underlying sperm maturation and capacitation are still not fully understood. Herein, we show that PPP3R2, a testis-specific regulatory subunit of protein phosphatase 3 (an isoform of calcineurin in the testis), is essential for sperm maturation and capacitation. Knockout of *Ppp3r2* in mice leads to male sterility due to sperm motility impairment and morphological defects. One very noteworthy change includes increases in sperm membrane stiffness. Moreover, PPP3R2 regulates sperm maturation and capacitation via (i) modulation of membrane diffusion barrier function at the annulus and (ii) facilitation of cholesterol efflux during sperm capacitation. Taken together, PPP3R2 plays a critical role in modulating cholesterol efflux and mediating the dynamic control of membrane remodeling during sperm maturation and capacitation.

Keywords: cholesterol metabolism, *Ppp3r2*, sperm deformity, sperm motility, sperm maturation

Introduction

In mammals, successful fertilization is dependent on sperm motility and fertility. These attributes develop subsequent to sperm exiting from the testis, whereas during early development they are immotile and incapable of moving through the female reproductive tract to induce fertilization. To acquire progressive motility and fertility competence, sperm need to undergo two post-testicular maturation processes, i.e. the one occurring in the male epididymis is known as epididymal sperm maturation and the other is designated as capacitation expressed in the female reproductive tract (Freitas et al., 2017). On the other hand, both of these changes are associated with sequential biochemical changes occurring in different sperm segments (Freitas et al., 2017; Gervasi and Visconti, 2017; Puga Molina et al., 2018). More specifically, during epididymal sperm maturation, mixing of sperm and epididymal luminal contents markedly changes sperm composition including both their protein makeup and membrane physicochemical properties. Such interchange is particularly facilitated via the epididymosomes or the epididymal proteins secreted by epididymal epithelia (Dacheux and Dacheux, 2013; Martin-DeLeon, 2015). In recent years, some studies characterized the mechanism of sperm epididymal maturation by focusing on the role of cyclic adenosine monophosphate (cAMP) signaling based on measurements of changes in intracellular cAMP content and subsequent protein kinase A (PKA) activity as well as changes in the phosphorylation status of numerous other proteins. Changes in phosphatase and glycogen synthase kinase 3 activity were also evaluated since they affect sperm acquiring progressive motility and fertility competence (Freitas et al., 2017; Gervasi and Visconti, 2017). Nevertheless, despite undergoing these developmental changes, mature sperm are still unable to fertilize oocytes immediately after ejaculation, because sperm motility and fertility development occur

Received May 5, 2019. Revised September 5, 2019. Accepted November 27, 2019.

only after they undergo another series of physiological modifications inside the female reproductive tract, collectively known as capacitation. At the molecular level, capacitation is associated with a series of events, including cAMP/PKA pathway activation, membrane cholesterol depletion that both increases membrane fluidity, protein tyrosine phosphorylation, intracellular pH alkalinization, Ca^{2+} signaling, membrane potential difference hyperpolarization, as well as changes in sperm plasma content (Whitfield et al., 2015; De Jonge, 2017; Puga Molina et al., 2018).

Protein phosphorylation status changes of either the serine/threonine or tyrosine residues are crucial to mediating both sperm maturation and capacitation, although such modification occurs at different sites (Dacheux and Dacheux, 2013; Freitas et al., 2017). During epididymal maturation, the increases of cAMP/PKA-dependent protein tyrosine phosphorylation in sperm occur in concert with progressive increases in motility, which also sets the stage for subsequent capacitation and acrosome reaction (Dacheux and Dacheux, 2013; Vadnais et al., 2013). Conversely, the removal of phosphate groups by phosphatases has also been implicated in epididymal sperm maturation (Huang and Vijayaraghavan, 2004; Vijayaraghavan et al., 2007; Silva et al., 2014; Goswami et al., 2019). On the other hand, some studies have shown that sperm phosphoprotein phosphatase 1 catalytic subunit gamma 2 (PPP1CC2, also named PP1γM2) activity declines during epididymal maturation and is important in regulating sperm motility (Vijayaraghavan et al., 1996; Mishra et al., 2003; Goswami et al., 2019).

Recently, another Ca^{2+}–calmodulin-dependent serine/threonine phosphatase, phosphoprotein phosphatase 3 (also known as PP2B, an isoform of calcineurin in the testis) that contains a catalytic subunit (PPP3CC) and a regulatory subunit (PPP3R2), has been found to play a critical role in sperm epididymal maturation (Miyata et al., 2015). Calcineurin exists as a heterodimer composed of a catalytic subunit (57–61 kDa) and a regulatory subunit (19 kDa) (Klee et al., 1998). In mammals, three isoforms of the catalytic subunit (PPP3CA, PPP3CB, and PPP3CC) and two isoforms of the regulatory subunit (PPP3R1 and PPP3R2) have been identified (Klee et al., 1998; Rusnak and Mertz, 2000). Notably, PPP3CA, PPP3CB, and PPP3R1 are expressed ubiquitously, whereas PPP3CC and PPP3R2 are highly and uniquely expressed in mouse testis and sperm (Miyata et al., 2015). Lack of either PPP3CC or PPP3R2 in mice leads to male infertility associated with impaired hyperactivated motility in sperm because of stiffness in the flagellar midpiece (Miyata et al., 2015). However, the molecular mechanisms by which either PPP3CC or PPP3R2 regulates sperm quality during epididymal sperm maturation remain virtually unknown.

To address this question, herein, we chose the regulatory subunit (PPP3R2) of phosphoprotein phosphatase 3, which was not fully reported, as a target gene and engineered *Ppp3r2* knockout mice to explore its effects on protein phosphorylation status and membrane fluidity during sperm maturation. In addition, we investigated the role of PPP3R2 in inducing sperm motility and cholesterol efflux during sperm capacitation. We found that PPP3R2 activity contributes to modulating membrane

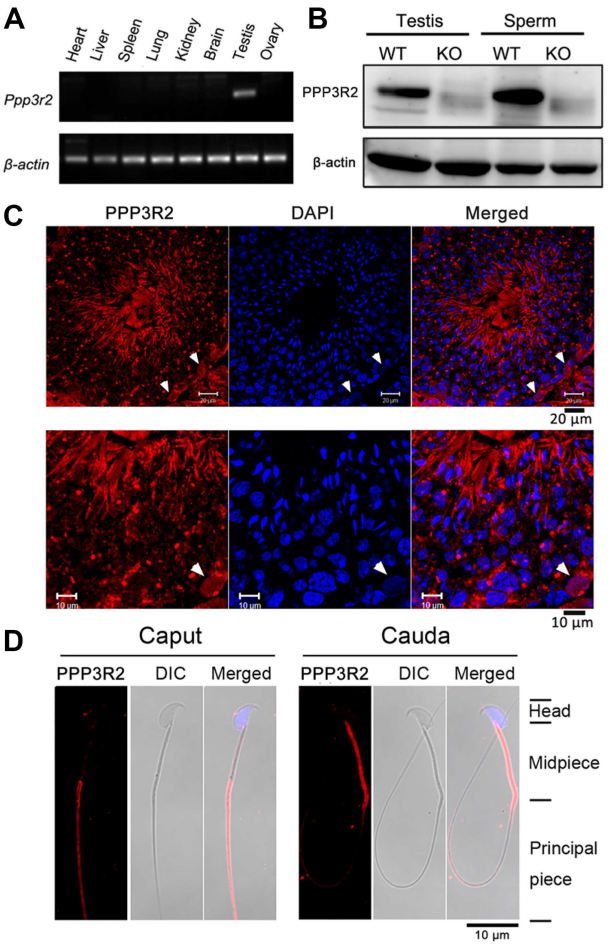

Figure 1 Tissue-specific PPP3R2 expression levels. (**A**) *Ppp3r2* mRNA expression in the heart, liver, spleen, lung, kidney, brain, testis, and ovary. RT-PCR results indicate higher *Ppp3r2* expression in the testis. *β-actin* expression validates loading equivalence. (**B**) Western blot analysis of testis and sperm PPP3R2 (21 kDa) expression in *Ppp3r2* KO mice reveals its absence, whereas it is apparent in their WT counterpart. (**C**) Immunofluorescent staining shows that PPP3R2 expression is localized in the germ cells of mouse testis. Arrows indicate its expression in spermatogonia. Scale bar, 20 μm (main) and 10 μm (enlarged). (**D**) Sperm PPP3R2 immunofluorescent staining is localized in the principal piece and midpiece originating from caput and cauda epididymis, respectively. DIC: differential interference contrast image. Scale bar, 10 μm.

diffusion barrier integrity at the annulus through septin 4 (Sept4) polymerization. Such PPP3R2 activity also promotes cholesterol efflux afforded by the ATP-binding cassette transporter 1 (ABCA1), which is involved in both sperm maturation and subsequent capacitation.

Results

PPP3R2 uniquely expresses in mouse testis and sperm

Western blot analysis identified the novel expression of PPP3R2 in mouse testis (Miyata et al., 2015). Herein, we used

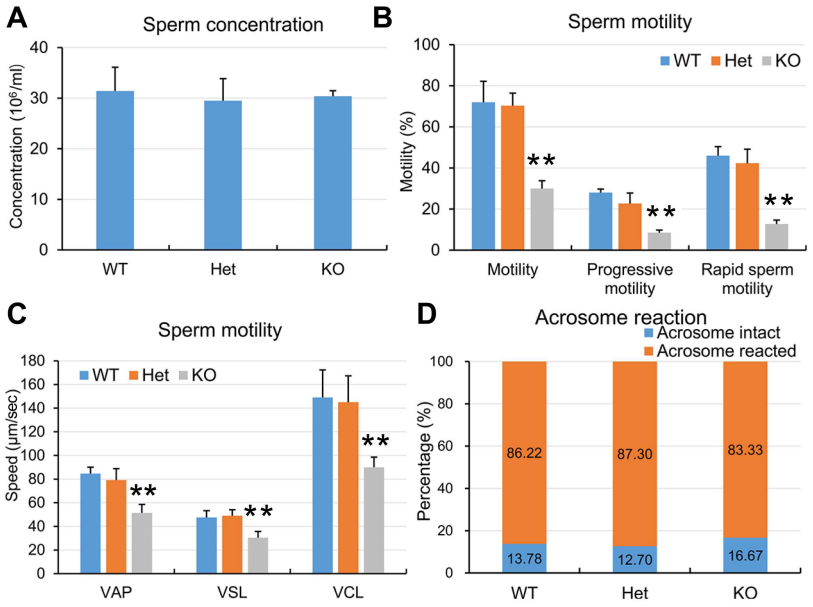

Figure 2 WT and *Ppp3r2* KO sperm quality analyses. (**A**) CASA of sperm concentration from cauda epididymis reveals no significant difference among WT, Het, and *Ppp3r2* KO mice. Error bars represent SD ($n = 8$). (**B** and **C**) CASA shows that sperm motility, progressive motility, and rapid sperm motility (**B**) as well as motile sperm speed (**C**) in *Ppp3r2* KO mice are greatly reduced compared to those in WT and Het mice. Error bars represent SD ($n = 8$). $^{**}P < 0.01$. (**D**) PNA staining shows acrosome reaction capacity induced by A23187, showing that this response in *Ppp3r2* KO sperm is similar to that in WT and Het sperm ($n = 8$).

PCR, immunohistochemistry, and immunoblotting to investigate the expression pattern of PPP3R2 in mouse testis and sperm. PCR analysis indicated that *Ppp3r2* mRNA was uniquely expressed in the testis (Figure 1A), and immunoblotting analysis also showed the expression of PPP3R2 in the testis and the mature sperm (Figure 1B). Immunofluorescence analysis revealed that PPP3R2 was expressed in spermatogonia, spermatocytes, and spermatids in the seminiferous epithelium (Figure 1C). Moreover, during epididymal maturation, the localization of PPP3R2 unexpectedly shifted on the sperm flagellum, from the principal piece of caput epididymal sperm into the midpiece of cauda epididymal sperm (Figure 1D; Supplementary Figure S1B).

Infertility, high sperm deformity, and low sperm motility in Ppp3r2 knockout mice

Ppp3r2 knockout (KO) male mice were healthy without any pathological changes in most principal organs and the testis (Supplementary Figure S2). In *Ppp3r2* KO mice, western blot analysis showed that PPP3R2 expression was absent in both the testis and sperm, confirming *Ppp3r2* gene knockout in these mice (Figure 1B). Additionally, male mice were completely infertile, whereas females had no fertility defects. This phenotypic difference is consistent with a previous report (Miyata et al., 2015).

To determine the cause of the male infertility in *Ppp3r2* null mice, their reproductive phenotype was assessed by computer-assisted sperm analysis (CASA) and morphological analysis. Homozygous KO male mice had normal-sized testes containing various types of developing germ cells in the seminiferous epithelium detected by hematoxylin and eosin (H&E) staining (Supplementary Figure S2). However, electron micrographs showed that there were some asyntactic spermatogonia located along the basal region of the seminiferous epithelium in the testis (Supplementary Figure S3). Despite these changes, the spermatogenesis was not disrupted. Accordingly, the testis still produced sufficient amounts of sperm, which afterwards were able to move to the caudal epididymis (Figure 2A).

During capacitation *in vitro*, it is also apparent that sperm motility (i.e. the percentage of motile sperm, progressive sperm, and rapid sperm) was significantly reduced in *Ppp3r2* KO mice than that in wild-type (WT) and heterozygote (Het) males (Figure 2B). More importantly, the speed of motile sperm, including average path velocity (VAP), straight-line velocity (VSL), and curvilinear velocity (VCL), was also significantly decreased in *Ppp3r2* KO mice (Figure 2C), but the ratios of sperm acrosome reaction induced by the Ca^{2+} ionophore A23187 were similar among WT, Het, and *Ppp3r2* KO males (Figure 2D).

Notably, sperm morphological deformity ratios were high in the sperm head, neck, and tail in *Ppp3r2* KO mice (Figure 3A). This ratio increased to reach 79.7% ± 4.6% in *Ppp3r2* KO mice compared to 19.3% ± 1.5% in WT mice (Figure 3A and B). Specifically, 37.6% had sperm tail deformity along with hairpin bending or breaking at the annulus of sperm tails (Figure 3B). On the other hand, both fluorescent axonemal staining by α-tubulin and electron microscopic analyses revealed an axonemal breakage at the junction between midpiece and principal piece (Figure 3C and D), which is designated as the annulus.

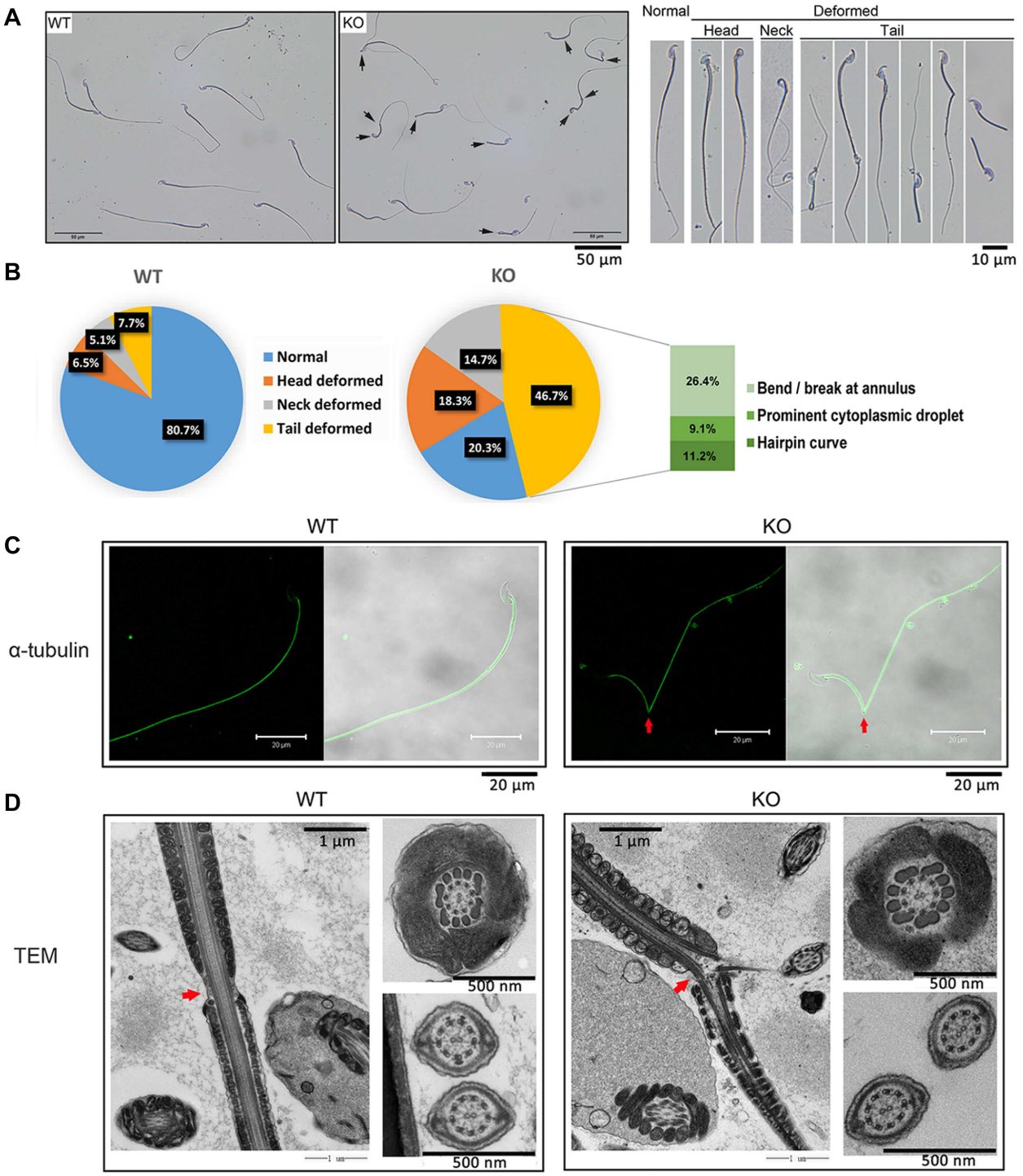

Figure 3 Loss of PPP3R2 induces sperm morphology deformity. (**A**) Compared to WT, *Ppp3r2* KO mouse sperm morphology has prominent deformities in the sperm head, neck, and mostly tail (arrows indicate deformed sperm). Scale bar, 50 μm. (**B**) Deformed sperm ratios calculated from eight independent experiments and each composed of at least 200 spermatozoa. Increased sperm deformity is evident in *Ppp3r2* KO mice, especially a high proportion of sperm possess bends in the annulus, cytoplasmic droplet, and hairpin curve. (**C**) Immunofluorescent staining of α-tubulin shows that the axoneme sperm tail is bent in *Ppp3r2* KO sperm (arrows indicate annulus bent sites). Scale bar, 20 μm. (**D**) Transmission electron micrograph analysis of sperm tails shows axonemal bending at the annulus (arrows) in *Ppp3r2* KO sperm, whereas the mitochondrial sheath, outer dense fiber, and axoneme in *Ppp3r2* KO sperm are normal. Scale bar, 1 μm (main) and 500 nm (enlarged).

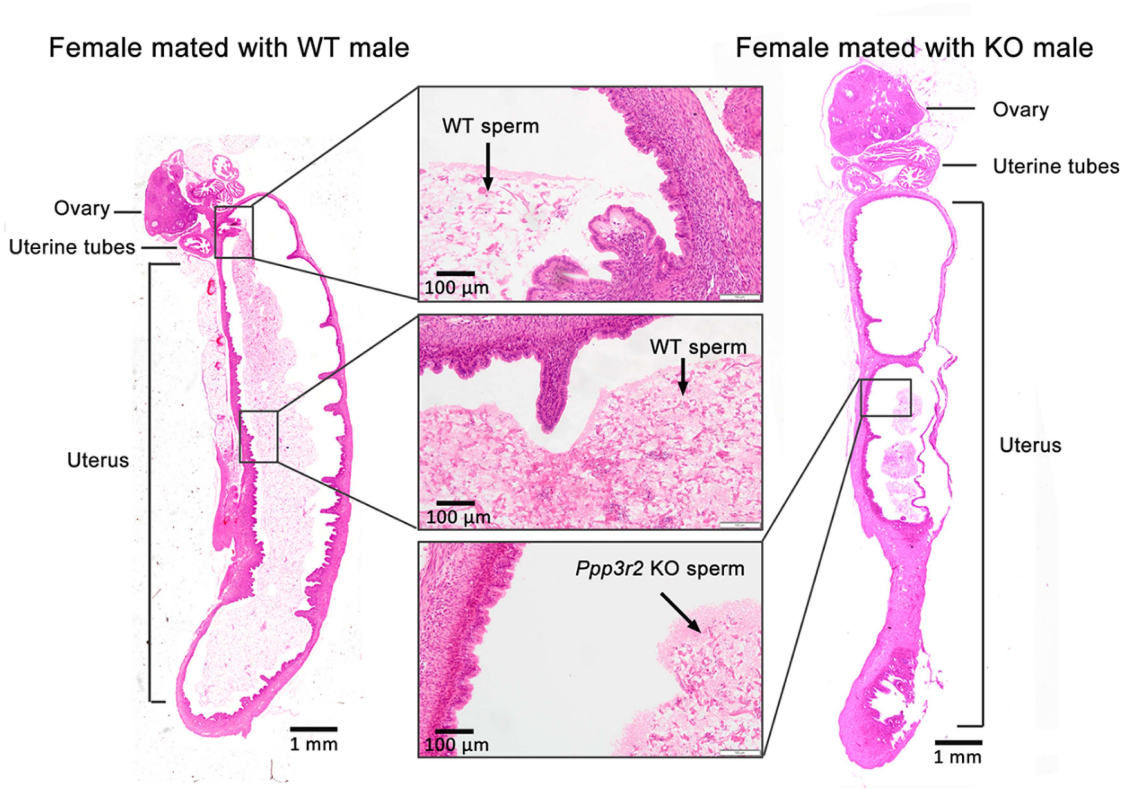

Figure 4 Tracking sperm movement in the reproductive tract after mating. WT and *Ppp3r2* KO males mated with fertile females, respectively; 12 h later, H&E staining identified sperm in uterine sections. WT sperm are dispersed in the whole uterus and some reach the uterine tubes, whereas *Ppp3r2* KO sperm accumulate at the front part of the uterus. Each group is consistently composed of three males. Scale bar, 1 mm.

However, there were no significant differences in immature sperm purified from the caput epididymis in sperm tail deformity between *Ppp3r2* KO and WT mice (Supplementary Figure S4).

Additionally, sexually mature healthy females were mated with either WT males or *Ppp3r2* KO males, and then the sperm in the female reproductive tract were examined. The results showed that WT sperm migrated through the uterus at variable speeds and some even successfully reached the uterine tubes, whereas *Ppp3r2* KO sperm mostly accumulated at the front part of the uterus (Figure 4). Thus, taking into account the greatly impaired sperm motility and morphology in *Ppp3r2* KO mice, poor sperm motility acquired during capacitation likely accounts for male infertility.

Unchanged levels of gonadal hormones, anti-sperm antibody, and inflammatory cytokines upon the loss of Ppp3r2

Poor sperm motility and abnormal morphology are common consequences of hormonal imbalance, oxidative stress, and inflammation, which are mainly caused by environmental stresses or pathophysiological changes due to obesity, infection, autoimmune reactions, etc. In order to identify the cause of sperm dysfunction in *Ppp3r2* KO mice, we evaluated the levels of gonadal hormones and anti-sperm antibody in mouse serum and inflammatory cytokines in the testis and epididymis. The results showed that the levels of testosterone, estradiol, and anti-sperm antibody in *Ppp3r2* KO mouse serum were not different from those in WT males (Supplementary Figure S5A and B). Similarly, the levels of proinflammatory cytokines IL-1β, IL-6, and TNF-α in the testis and epididymis were not different between WT and *Ppp3r2* KO groups (Supplementary Figure S5C and D). Therefore, *Ppp3r2* absence did not alter gonadal hormone and proinflammatory cytokine expression levels. Instead, loss of phosphatase activity seems to affect sperm function.

Ppp3r2 deficiency lowers intracellular cAMP concentration and Ca^{2+} levels in sperm

In *Ppp3r2* KO caudal sperm, the cAMP content was lower than that in WT sperm (Figure 5A). However, supplementation with dibutyryl cAMP (db-cAMP), a cell-permeable cAMP analogue that activates PKA, failed to rescue the low motility of *Ppp3r2* KO sperm (Figure 5B). Similarly, intracellular Ca^{2+} content, characterized as a main regulator of both sperm motility and acrosome reaction, also fell in *Ppp3r2* KO caudal sperm (Figure 5C). Moreover, raising intracellular Ca^{2+} levels with a low concentration of A23187, a calcium ionophore, partially promoted sperm motility but did not alter progressive motility and rapid motility after 30-min treatment of *Ppp3r2* KO caudal sperm (Figure 5D). Despite A23187 treatment, *Ppp3r2* KO caudal sperm motility

was still much lower than that in WT sperm (Figure 5D). Thus, there were no significant effects on the sperm motility with cAMP and Ca^{2+} supplementation, suggesting that the signaling pathway events compromised by the loss of *Ppp3r2* function are complex.

Ppp3r2 deficiency impairs membrane diffusion during epididymal maturation

Since both epididymal sperm maturation and subsequent capacitation are dependent on calcineurin activity, changes in protein phosphorylation status due to the loss of *Ppp3r2* function may alter these transitions. Based on this supposition, we sought to identity the key PPP3R2 targets whose modulations affect sperm maturation. Sept4 may be a candidate target for PPP3R2, for the phenotype of *Septin4* knockout mice shares many of the characteristics of *Ppp3r2* knockout mice, including male sterility and sperm tail hairpin bending (Kissel et al., 2005). Sept4 is a filament-forming GTPase, and its polymerization is necessary for the formation of a membrane diffusion barrier at the annulus, a cortical ring separating the midpiece and principal piece of the sperm tail. Its integrity is essential for restricting the localization of membrane proteins, including Basigin. In WT mice, Sept4 displayed restricted localization in the annulus. Accordingly, Basigin is confined to the principal piece in caput sperm and then relocates to the midpiece during sperm epididymal maturation (Figure 5E). However, in *Ppp3r2* KO sperm, Sept4 localization was no longer restricted to the annulus. It was instead dispersed to the midpiece of sperm flagella in either caput or cauda sperm. Such redistribution indicates impaired barrier function at the annulus. Thus, in *Ppp3r2* KO mice, sperm exhibited normal Basigin localization in caput sperm. However, this limited Basigin expression in their midpiece was lost during epididymal transit toward the cauda (Figure 5E), which coincides with impaired barrier function at the annulus in *Ppp3r2* KO sperm.

Ppp3r2 deficiency impairs cholesterol efflux and reduces sperm membrane fluidity

Since low track speed and midpiece bending increased in *Ppp3r2* KO sperm during capacitation *in vitro*, these effects suggested that increases in membrane rigidity hinder sperm flagella hyperactivation. Accordingly, we hypothesized that impaired cholesterol efflux during capacitation lowers membrane fluidity and increases sperm rigidity, which in turn decreases sperm motility in *Ppp3r2* KO mice. Other effects consistent with the decreases in sperm motility are the declines in ABCA1 content as well as its phosphorylation status during capacitation (Figure 6A and B). Since ABCA1 mediates net cholesterol efflux across the sperm membrane, these changes reduce sperm membrane fluidity during capacitation in *Ppp3r2* KO caudal sperm. Such dependence of cholesterol efflux on functional *Ppp3r2* expression is also supported by the finding that cholesterol concentration in *Ppp3r2* KO sperm was unaltered during capacitation, whereas it fell significantly in WT sperm during the same time (Figure 6C). Since most (~90%) of the cholesterol content is located in the plasma membrane (Leahy and Gadella, 2015), this result supports the notion that *Ppp3r2* deficiency reduced cholesterol efflux across the sperm membrane during capacitation. Furthermore, sperm membrane cholesterol stained by the fluorescent probe filipin (Takeo et al., 2008) and evaluated by flow cytometry analysis also indicated that the cholesterol level in *Ppp3r2* KO sperm was significantly higher than that in WT sperm after capacitation (Figure 6D). On the other hand, lipid rafts constitute a distinct membrane subdomain enriched in cholesterol. They are composed of the multifunctional scaffolding protein caveolin-1, which is a definitive biomarker of lipid rafts (Bickel et al., 1997; Smart et al., 1999). In agreement with the lack of change in cholesterol levels in *Ppp3r2* KO sperm, caveolin-1 content immunoblotting analysis showed that its level was little changed during capacitation, whereas it decreased significantly in WT sperm during the same time (Figure 6E). In parallel, immunofluorescent staining showed that caveolin-1 was localized mainly in the acrosome and midpiece of the mature sperm. Its expression essentially disappeared during capacitation in WT sperm, whereas its pattern was unchanged during this phase in *Ppp3r2* KO sperm (Figure 6F). This near invariance in lipid structure is also in agreement with decreased cholesterol efflux since this steroid constitutes most of the structural framework of lipid rafts.

We also evaluated plasma membrane fluidity changes during capacitation using merocyanine 540 (M540). This methodology targets membrane fluid domains and evaluates membrane lipid order (Gillan et al., 2005; Martin et al., 2005). Using flow cytometry analysis, a high percentage of WT sperm exhibited a strong M540 fluorescence signal during capacitation for 10 and 30 min, whereas M540 staining intensity in *Ppp3r2* KO sperm was significantly less, which is indicative of a lower proportion of sperm undergoing capacitation (Figure 6G).

Therefore, these results suggest that increases in cholesterol efflux occurring during early capacitation were disrupted in *Ppp3r2* KO sperm. This suppression decreased membrane fluidity and presumably contributed to impairing sperm movement.

Calcineurin inhibition impairs sperm motility and promotes sperm deformity through declines in membrane fluidity and PKA activity in vivo

To provide additional evidence that *Ppp3r2* supports expression of sperm quality, we determined the effects of cyclosporine A (CsA), a calcineurin inhibitor, on sperm behavior in WT mice. Since it takes ~10 days for sperm to transit to the epididymis, CsA treatment lasting 2 weeks was assumed to be long enough to determine whether calcineurin is involved in mediating epididymal maturation (Miyata et al., 2015). Indeed, such treatment changed their sperm behavioral parameters. They became similar to those seen in *Ppp3r2* KO mice. Specifically, the percentage of the motile sperm that exhibited progressive and rapid sperm movement significantly decreased in CsA-treated WT mice in comparison to those in their untreated counterpart (Figure 7A). Meanwhile, sperm from CsA-treated

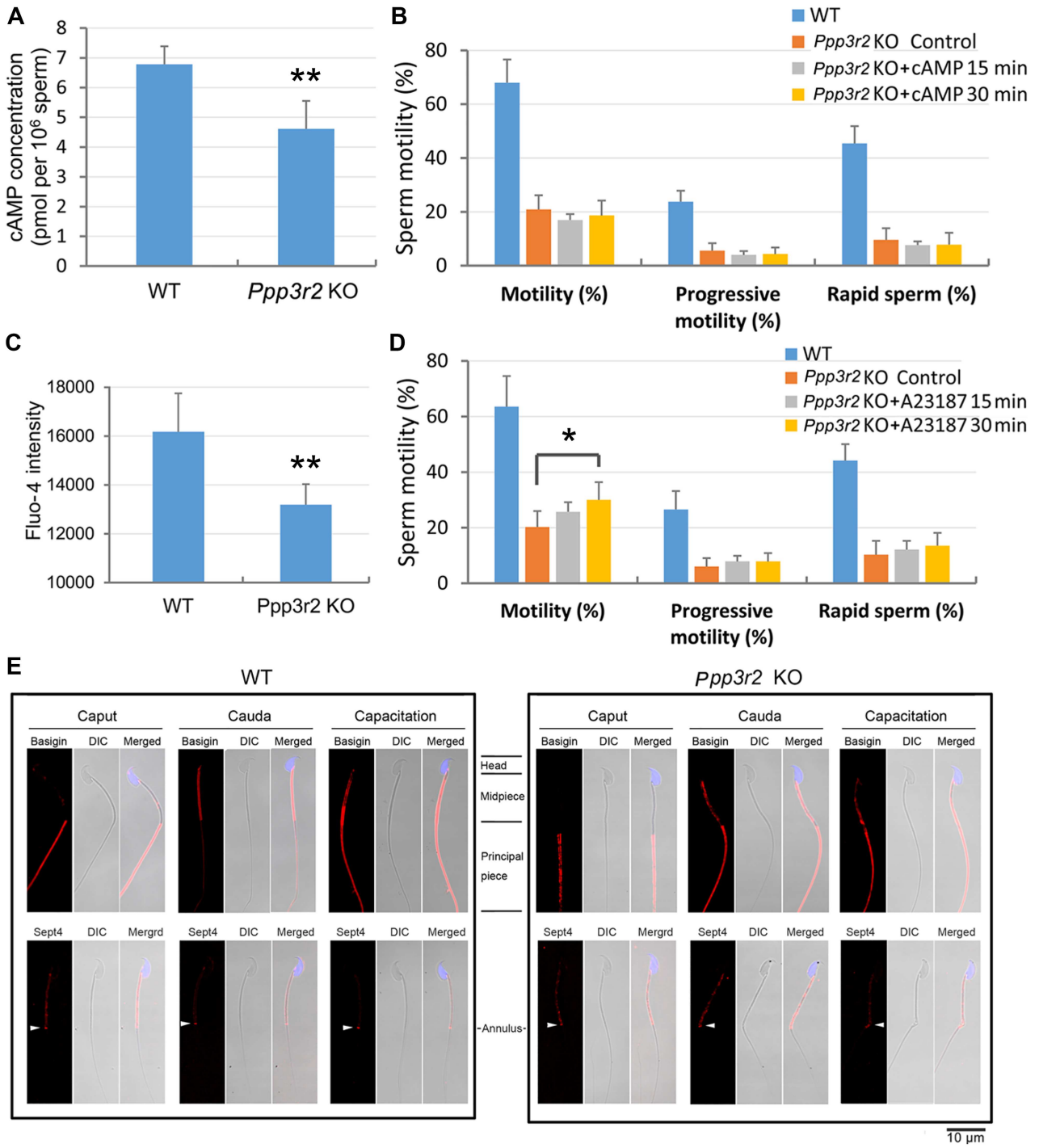

Figure 5 Loss of PPP3R2 function reduces cAMP and calcium levels in sperm and compromises membrane diffusion during sperm maturation. (**A**) cAMP concentration declines in *Ppp3r2* KO sperm. Error bars represent SD ($n = 8$). $^{**}P < 0.01$. (**B**) db-cAMP supplementation fails to reverse sperm motility decrement in *Ppp3r2* KO sperm. Error bars represent SD ($n = 7$). (**C**) Calcium level, determined by Fluo-4 staining and flow cytometry, decreases in *Ppp3r2* KO sperm. Error bars represent SD ($n = 8$). $^{**}P < 0.01$. (**D**) A23187 treatment fails to restore *Ppp3r2* KO sperm motility to a normal level of WT sperm even though transiently increased for 30 min. Error bars represent SD ($n = 7$). $^{*}P < 0.05$. (**E**) Immunofluorescent staining of Basigin and Sept4 in sperm during epididymal transit and capacitation: in WT mice, Basigin is localized in the principal piece of caput epididymis, and after epididymal transit, its localization is restricted to the midpiece of cauda epididymis sperm. Ultimately, it is localized in the whole tail after capacitation, whereas in the *Ppp3r2* KO mice, Basigin localization pervades throughout the whole tail of cauda epididymis sperm. Sept4 expression is limited to the annulus (arrows) in WT sperm but is dispersed in *Ppp3r2* KO sperm. These results suggest that loss of diffusion barrier integrity occurs specifically in the cauda epididymis. Scale bar, 10 μm.

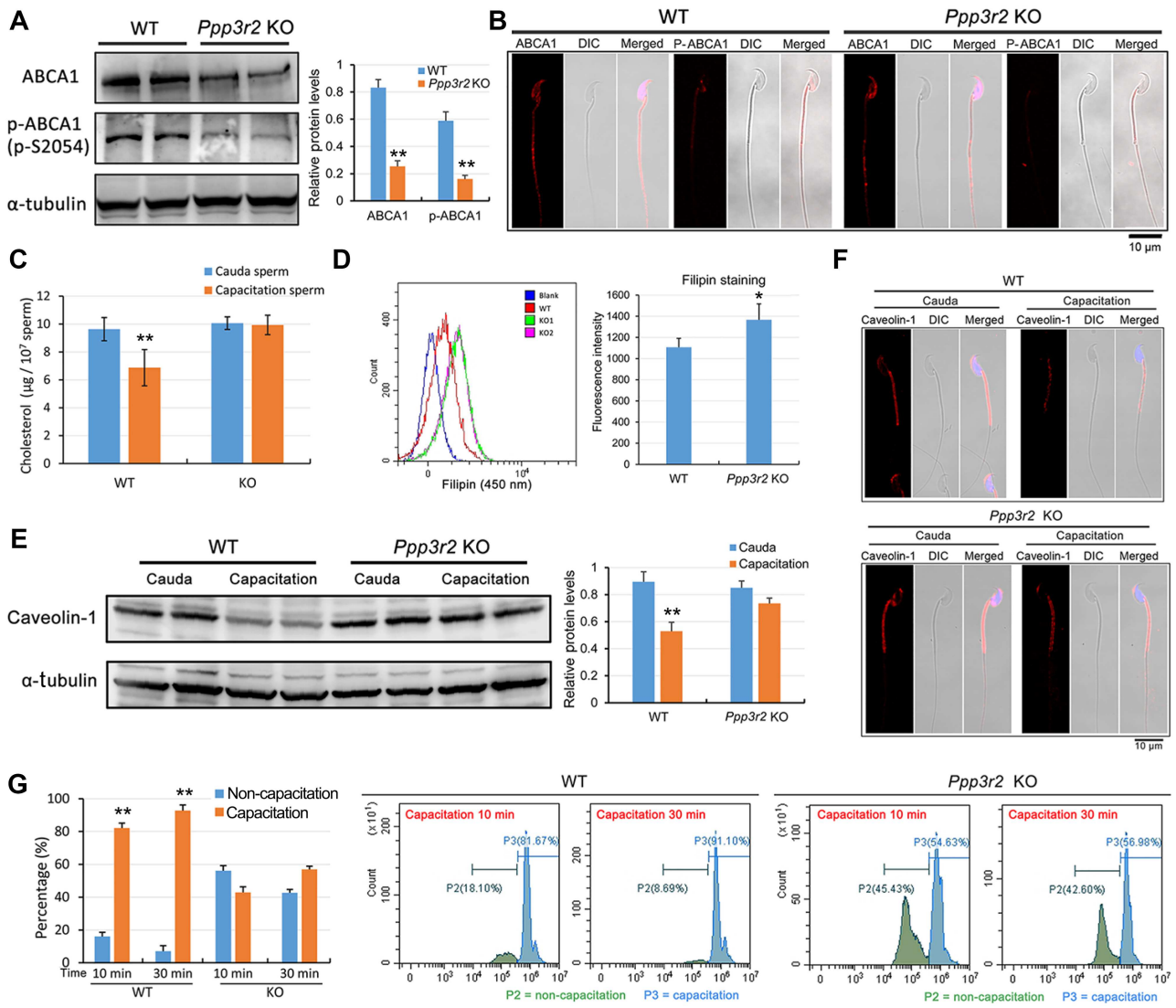

Figure 6 Loss of PPP3R2 function disrupts ABCA1-dependent cholesterol efflux and decreases membrane fluidity. (**A** and **B**) ABCA1 western blot analysis (**A**) and immunofluorescent staining (**B**) show reduced ABCA1 expression and phosphorylated ABCA1 content in *Ppp3r2* KO sperm. α-tubulin expression validates loading control equivalence. Scale bar, 10 μm. (**C**) Sperm cholesterol assay shows decreased cholesterol content in WT sperm after capacitation, whereas cholesterol efflux is impaired in *Ppp3r2* KO sperm during capacitation. Error bars represent SD ($n = 5$). $^{**}P < 0.01$. (**D**) Flow cytometry analysis of up-swim sperm stained by the membrane cholesterol probe filipin indicates significantly high fluorescent staining of filipin in *Ppp3r2* KO sperm compared to WT sperm. Error bars represent SD ($n = 7$). $^{*}P < 0.05$. (**E** and **F**) Western blot analysis (**E**) and immunofluorescent staining (**F**) of caveolin-1 indicate cholesterol-enriched lipid rafts within the sperm membrane. The results show decreased caveolin-1 content in WT sperm after capacitation, whereas it changes little in *Ppp3r2* KO sperm during capacitation. Scale bar, 10 μm. (**G**) Sperm membrane fluidity evaluated by M540 staining and flow cytometry analysis. Intense M540 staining represents good membrane fluidity characteristic of capacitation, which is evident in WT sperm, whereas only a small proportion of *Ppp3r2* KO sperm undergo capacitation. Error bars represent SD ($n = 5$). $^{**}P < 0.01$.

mice exhibited a high ratio of sperm tail deformity (tail deformity 51.3%, Figure 7B). They also displayed either hairpin bending or breakage at the annulus of the sperm tails (Figure 7C). More importantly, membrane fluidity evaluated by M540 staining also significantly declined in sperm from CsA-treated mice, and the proportion of capacitated sperm was less than that from untreated WT controls (Figure 7D and E). Western blot analysis also showed that the expression levels of both total ABCA1 and phosphorylated ABCA1 declined in CsA-treated sperm during capacitation (Figure 7F).

Furthermore, changes in calcineurin activity usually affect the PKA signaling pathway (Lester et al., 2001; Dell'Acqua et al., 2006; Voss et al., 2010; Dittmer et al., 2014). Herein, western blot analysis indicated that the phosphorylated PKAR2

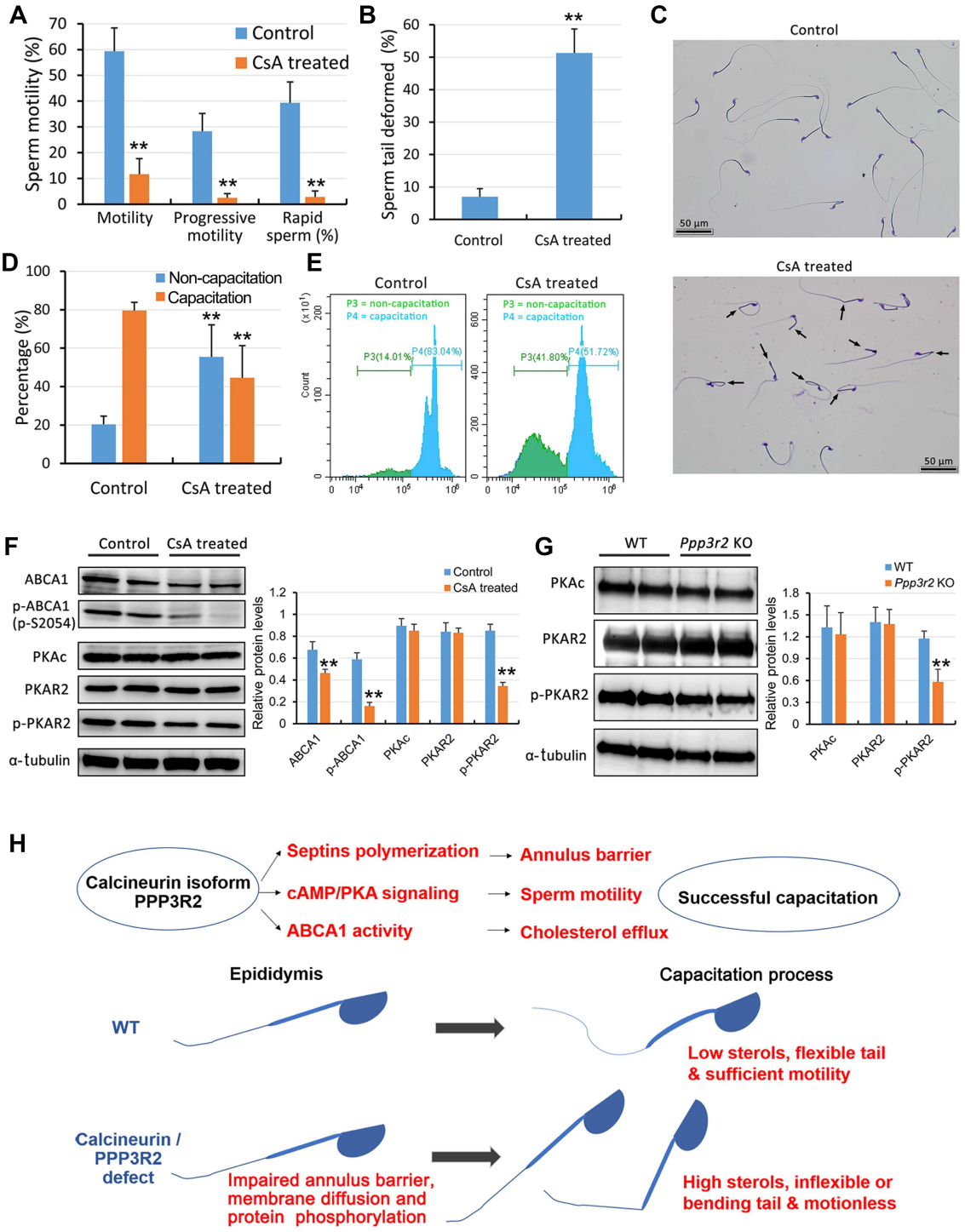

Figure 7 CsA treatment reduces sperm quality. (**A**) CASA shows that CsA treatment for 2 weeks suppresses sperm motility, progressive motility, and rapid sperm motility. Error bars represent SD (n = 5). $^{**}P < 0.01$. (**B** and **C**) Sperm morphology analysis reveals that CsA treatment induces prominent sperm tail deformity, because bends and hairpin curves develop at the annulus (arrows). Sperm tail deformity was calculated from five independent experiments in both control and CsA-treated mice, and at least 200 spermatozoa were enlisted in each independent experiment. Error bars represent SD (n = 5). $^{**}P < 0.01$. Scale bar, 50 μm. (**D** and **E**) Sperm membrane fluidity evaluated by M540 staining intensity and flow cytometry analysis. CsA treatment does not increase the percentage of capacitated sperm with intense M540 staining occurring 30 min after capacitation, compared to untreated control sperm. This negative effect suggests that sperm membrane fluidity (capacitation) is significantly reduced after calcineurin is inhibited by CsA during epididymal transit. Error bars represent SD (n = 5). $^{**}P < 0.01$. (**F**) Western blot analysis shows reduced expression levels of ABCA1, phosphorylated ABCA1, and phosphorylated PKAR2 in CsA-treated sperm. (**G**) Western blot analysis shows reduced PKAR2 phosphorylation in *Ppp3r2* KO sperm. α-tubulin expression validates loading

(phosphor-S99), the regulatory subunit of PKA and a marker of activated PKA signaling, fell in both CsA-treated sperm and *Ppp3r2* KO caudal sperm (Figure 7F and G). These results suggest that both PPP3R2 inactivity and deficiency may disrupt the PKA signaling pathway and also inhibit downstream protein expression patterns in mature sperm.

Discussion

There is suggestive evidence that testis/sperm-specific isoforms of calcineurin including PPP3CC and PPP3R2 are crucial for maintenance of sperm motility and male fertility (Miyata et al., 2015). However, the underlying mechanisms are still poorly understood regarding how they contribute to the sperm maturation process. In the present study, the regulatory subunit *Ppp3r2* KO mice were generated in order to clarify how calcineurin supports the sperm maturation process. The results clearly show that calcineurin modulates both ABCA1 function and the net cholesterol efflux mechanism expression level by inducing changes in their phosphorylation status. Such regulation is important for mediating sperm maturation. This dependence is evident since poor sperm motility and sperm morphological defects, declines in cholesterol efflux and membrane fluidity, occurred in *Ppp3r2* KO sperm during epididymal maturation. Since all of these changes were similar to those occurring in WT mice treated with CsA, the activity of this phosphatase makes an essential contribution to supporting epididymal sperm maturation and fertility. This realization makes it evident that PPP3R2, which is the regulatory subunit of calcineurin, is crucial for providing its phosphatase activity and regulating epididymal sperm transit through controlling sperm protein phosphorylation status. Such control promotes formation of an effective membrane diffusion barrier at the annulus and supports activation of the cholesterol efflux mechanism in preparation for capacitation. Furthermore, such phosphatase activity optimizes sperm motility and natural fertility.

It is common knowledge that modulation of the protein phosphorylation status is particularly important in governing sperm function, because mature sperm cells are terminally differentiated cells and transcriptionally as well as translationally silent (Dun et al., 2012; Gervasi and Visconti, 2017). Phosphorylation events, at either serine/threonine or tyrosine residues, are generally linked with both sperm maturation and capacitation. Here, we found that modulation of protein phosphorylation status is associated with changes in sperm function, since a decline in phosphatase activity arising from *Ppp3r2* deficiency decreased sperm motility and fertility and altered sperm morphology. Such effects reduced sperm fertilization, which was mainly due to a lower ratio of motile sperm resulting from significantly lower sperm motor speed in *Ppp3r2* KO mice. On the other hand, the *Ppp3r2* KO sperm flagella were either bent or even broken during capacitation in Tyrode's buffer, whereas immature KO sperm isolated from the caput epididymis had the same properties as those in the WT sperm, suggesting that sperm deformities developed during epididymal transit in *Ppp3r2* KO mice. Accordingly, sperm morphological analysis showed severe hairpin bending in the flagella and even breaking at the annulus of sperm tails (~37.6%), hinting a conflict developed between the intrinsic motor of the activated sperm tails and the rigidly inflexible midpiece in *Ppp3r2* KO sperm. These effects were replicated during epididymal maturation in WT mice whose calcineurin function was blocked with CsA treatment. In addition, their phenotypes were the same as those in *Ppp3r2* KO sperm. Therefore, PPP3R2 expression is essential for endowing calcineurin with its phosphatase activity. Moreover, analysis of sperm migration in the female reproductive tract *in vivo* revealed that the poor motility of *Ppp3r2* KO sperm occurring in capacitation was primarily responsible for the infertility. These changes in *Ppp3r2* KO sperm were also described in *Ppp3cc* KO mice in which male infertility was evident along with poor sperm motility, low counts, and less acrosome reaction (Miyata et al., 2015). Hence, these results indubitably confirm that PPP3R2 expression is essential for developing sperm that are competent enough to induce fertilization.

Notably, some phosphatases, such as PPP1CC and PPP2CA, are crucial for spermatogenesis and male fertility (Chakrabarti et al., 2007; Forgione et al., 2010; Sinha et al., 2013; Pan et al., 2015). *Ppp1cc* or *Ppp2ca* knockout in germ cells impaired spermatogenesis associated with abnormal testicular morphology (Forgione et al., 2010; Pan et al., 2015). Although the previous study and our current results describe a relationship between PPP3R2/PPP3CC expression and sperm maturation during epididymal transit, some crucial ultrastructural alterations were evident in the seminiferous epithelium of *Ppp3r2* KO mice. In other words, despite PPP3R2 being expressed in spermatogonia, loss of *Ppp3r2* function resulted in the loss of part of the spermatogonia along with some variable-sized vacuoles remaining in the basal region of the seminiferous epithelium. This persistence of the spermatogenic process generating sperm in both testicular and epididymal lumens indicates that among numerous phosphatases in spermatogenic cells, either sperm calcineurin or its regulatory unit PPP3R2 plays a minor role in the maintenance of spermatogenesis. Nevertheless, PPP3R2 might instead have a more important regulatory role participating in sperm maturation during epididymal transit.

control equivalence in both **F** and **G**. Error bars represent SD ($n = 6$). $^{**}P < 0.01$. (**H**) Schematic representation of PPP3R2 function in sperm. In WT sperm, PPP3R2 modulates septin polymerization, cAMP/PKA signaling, and ABCA1 activity during epididymal sperm maturation. These functions support annulus barrier function, sperm motility, and cholesterol efflux during sperm capacitation in the female reproductive tract. Otherwise, PPP3R2 deficiency results in defective sperm maturation due to elevated membrane sterol levels. Such rises result in declines in membrane fluidity and membrane flexibility or tail bending, which accounts for poor sperm motility.

To clarify the underlying mechanism of PPP3R2 involvement in sperm maturation, we initially focused on the phosphorylation-related signaling pathways that mediate sperm motility. As predicted, cAMP and calcium levels were affected by the loss of *Ppp3r2* function. To confirm that declines in cAMP and calcium content were attributable to the absence of PPP3R2 expression, we performed rescue experiments by raising intracellular cAMP content and calcium levels through exposure to exogenous db-cAMP or A23187. However, they had little effect on promoting sperm motility, suggesting that loss of *Ppp3r2* function compromised other sperm structures or functions than merely inactivating cAMP and Ca^{2+} signal pathways in *Ppp3r2*-deficient sperm.

We sought to clarify the significance of deformed sperm morphology, which included annulus bending and flagella stiffness, in *Ppp3r2* KO sperm. The annulus is located at the midpiece–principal piece junction of the flagella, whereas little is known about its function in sperm. Some studies suggested that it may act as a diffusion barrier along the sperm flagella, or it may play a role in the formation of the mitochondrial array of the midpiece (Christova et al., 2004; Kissel et al., 2005). Sept4 and other septins are found in the annulus (Lin et al., 2011; Kuo et al., 2015), and Sept4 or Sept12 null sperm have an altered midpiece–principal piece junction and a hairpin formation at the annulus, which are similar to that found in *Ppp3r2* KO sperm (Ihara et al., 2005; Kissel et al., 2005; Kuo et al., 2012). Furthermore, the polymerizing function of either Sept4 or Sept12 is regulated by its phosphorylation status. Such control is crucial for forming a membrane diffusion barrier at the annulus. This realization suggests that either Sept4 or Sept12 dephosphorylation induces polymerization, whereas an increase in their phosphorylation status leads to the loss of the barrier function (Koch et al., 2015; Shen et al., 2017; Lin et al., 2019). Herein, our results suggested that Sept4 might be a PPP3R2 target, since polymerization of Sept4 at the annulus of *Ppp3r2*-deficient sperm was disrupted during epididymal transit. On the other hand, the abnormal shape of the annulus in *Ppp3r2* KO sperm suggests PPP3R2 may be involved in regulating the flagellar shape and dynamics of septin assembly, potentially by modifying its phosphorylation status. Thus, it is tenable that PPP3R2 deficiency could compromise the membrane diffusion barrier integrity and cause the loss of restricted protein localization in the sperm tail as well, which is possible as Basigin localization was disrupted in the flagellar membrane.

Sperm plasma membrane fluidity affects the fertilizing ability through controlling processes such as sperm maturation, capacitation, acrosome reaction, and sperm oocyte membrane fusion (Gadella and Boerke, 2016), whereas flagellar stiffness is associated with reduced sperm motile speed in *Ppp3r2* KO sperm. The effect caused by the loss of *Ppp3r2* function indicates that a hard-shelled membrane forms in the sperm tail. As activation of the cAMP/PKA signaling pathway upregulates tyrosine protein phosphorylation, this change is a hallmark of sperm capacitation and necessary for the acquisition of sperm fertilization competence (Vadnais et al., 2013; Puga Molina et al., 2018). However, less is known about specific phosphorylation events that occur during epididymal transit and how these events affect sperm maturation. For instance, we were unable to determine how PPP3R2 modulates the phosphorylation of sperm proteins and affects the membrane remodeling process during sperm maturation, which further confers on the sperm membrane the ability to undergo capacitation.

In most mammals, there is an average decrease in the cholesterol/phospholipid ratio between caput and cauda sperm plasma membranes. Cholesterol has a stabilizing effect on the plasma membrane by imposing conformational order on lipids. Decreased cholesterol elicits an increase in sperm plasma membrane fluidity during epididymal maturation (Rejraji et al., 2006; Saez et al., 2011; Gervasi and Visconti, 2017). Moreover, in some membrane microdomains within the whole sperm, cholesterol is enriched. Such rises result in decreases in membrane fluidity and increases in its rigidity. In these regions, the membrane is anisotropic due to lipid raft formation (Thaler et al., 2006; Gadella and Boerke, 2016). A number of sperm membrane proteins are constituents of the lipid raft. Some of them can directly bind to signal transducer proteins to act as scaffolds or foci for signaling pathways, thereby compartmentalizing specific pathways to specific regions in sperm (Simons and Toomre, 2000; Foster et al., 2003; Cross, 2004; Bou Khalil et al., 2006; Watanabe and Kondoh, 2011). Lipid raft function appears to be essential for numerous biological processes regulating sperm capacitation as well as subsequent fertilization. Additionally, cholesterol is a powerful decapacitation factor that serves to stabilize the sperm plasma membrane during epididymal transit and prevents the intermolecular interactions responsible for achieving a capacitated state (Travis and Kopf, 2002; Leahy and Gadella, 2015). Therefore, increases in cholesterol efflux out of the lipid rafts augments membrane fluidity. Such rises facilitate activation of effector enzymes like adenylyl cyclase linked to signaling pathways and in turn stimulate net ion transporter activity (Travis and Kopf, 2002). For instance, during sperm capacitation, an increase in cholesterol efflux from the mature sperm membrane is involved in activating the cholesterol efflux transporter such as ABCA1. Furthermore, cAMP/PKA signaling enhancement can increase the ABCA1 phosphorylation status and in turn promote cholesterol efflux. This effect increases membrane fluidity, which in turn enhances the biological activity of sperm surface proteins (Selva et al., 2004; Morales et al., 2008; Hu et al., 2009; Palme et al., 2014). Herein, we found that *Ppp3r2* deficiency could impair PKA activity, which in turn may reduce both sperm ABCA1 content and its phosphorylation status. These effects are associated with decreases in membrane diffusion barrier function at the annulus. Such changes restrict protein translocation and net cholesterol efflux, which in turn decreases membrane fluidity.

It should be emphasized that an increase in plasma membrane fluidity is one of the first changes involved in capacitation, which is associated with removal of cholesterol from the plasma membrane, leading to rearrangement of phospholipids (Aitken and Nixon, 2013). The fluorescent dye M540 allegedly progressively augments cell membrane staining intensity as its lipid

components become more disordered. Thus, M540 staining was used to evaluate the early events of capacitation in live unfixed sperm (Gillan et al., 2005; Martin et al., 2005). These attributes account for why it was used here to mainly evaluate sperm membrane destabilization. Sperm from both *Ppp3r2*-deficient mice and CsA-treated mice exhibited low M540 staining, suggesting poor membrane fluidity and a capacitation defect in these sperm. Meanwhile, cholesterol content and lipid raft distribution in *Ppp3r2*-deficient sperm were reduced less during capacitation than in the WT counterpart. This difference is consistent with less M540 staining, indicating less membrane fluidity paralleled by impaired cholesterol efflux.

In mouse sperm, ATP-binding cassette transporters, such as ABCA1, ABCA7, and ABCG1, mediate plasma membrane cholesterol efflux during their maturation and capacitation (Morales et al., 2008). In this study, we found that ABCA1 expression, rather than ABCA7 or ABCG1, declined in *Ppp3r2*-deficient sperm (Supplementary Figure S6). Although the underlying mechanism of this differential expression is unclear, it is possible that the ABCA1 phosphorylation status may be more susceptible to changes in the related signaling activity mediating control of this condition. For instance, ABCA1 expression and phosphorylation are known to be activated by cAMP/PKA signaling (Lawn et al., 1999; Oram et al., 2000; Haidar et al., 2002; Haidar et al., 2004; Hu et al., 2009; Nishiuchi et al., 2010). Moreover, liver X receptor-deficient male mice, which are infertile owing to disordered cholesterol homeostasis in the epididymis, have a specific loss of ABCA1 expression in the apical cells of the proximal caput epididymis. On the other hand, the expression levels of two other cholesterol transporters (ABCG1 and scavenger receptor B1) undergo little change (Ouvrier et al., 2009).

Interestingly, several studies showed that calcineurin inhibition decreased ABCA1-dependent cholesterol efflux (Le Goff et al., 2004; Karwatsky et al., 2010; Nagao et al., 2013). Herein, we presume that ABCA1 is a major cholesterol efflux transporter since ABCA1-deficient mice were less fertile possibly as a result of altered lipid levels in sperm (Selva et al., 2004). This mechanism may be an important factor supporting sperm capacitation and fertility. Thus, in the present study, the phosphorylation status of ABCA1 decreased in *Ppp3r2*-deficient sperm, which was accompanied by increased retention of cholesterol and lipid rafts and reduced membrane fluidity in both mature sperm and capacitated sperm. Therefore, impaired cholesterol efflux might directly impede sperm capacitation and contribute to the defects in both sperm motility and morphology in *Ppp3r2*-deficient sperm.

Taken together, we show here that the regulatory role of PPP3R2 expression and its protein phosphorylation status are both essential for modulating dynamic membrane remodeling via controlling membrane cholesterol efflux during sperm maturation and capacitation (Figure 7H). Accordingly, PPP3R2 expression is crucial for sustaining sperm maturation commensurate with sperm health and male fertility. Therefore, developing ligands that selectively target PPP3R2 expression may provide novel options for treating male infertility and improving the effectiveness of contraceptive pills.

Materials and methods

Animals

C57BL/6 mice (8–10 weeks old) were purchased from Shanghai Laboratory Animal Center. *Ppp3r2* KO mice were purchased from Velocigene, Inc. and the details of the mice are accessible online (http://www.velocigene.com/komp/detail/10637). *Ppp3r2* homozygous (knockout) mice and their WT littermate controls were produced by intercrossing *Ppp3r2* heterozygous mice. All of the mice were acclimated, interbred, and maintained under pathogen-free conditions in the Animal Center of Shanghai Jiao Tong University School of Medicine. On the other hand, all mice were housed in a temperature- and humidity-controlled room on a 12-h light–dark cycle and provided with ad libitum access to water and food. Animal experiments were conducted according to the International Guiding Principles for Biomedical Research Involving Animals, as promulgated by the Society for the Study of Reproduction. This research program was approved by the ethics committee of Shanghai Jiao Tong University School of Medicine (No. A2015-034).

Tissue and sperm preparation

Mice were euthanized with CO_2, and then their tissues were removed. For RNA and protein analyses, tissues were immediately lysed or snap frozen in liquid N_2. For histological analysis, tissues were fixed overnight either in Bouin's solution or in 2.5% glutaraldehyde buffer for electron microscopy analysis. Mature sperm were collected from the caudal epididymis by centrifugation in a 45% Percoll gradient (GE Healthcare) (800 *g*, 20 min, 4°C) and then washed thrice with PBS.

Ppp3r2 expression in tissues identified by RT-PCR

Tissues were homogenized in the TRIzol reagent (Invitrogen). cDNA was prepared from 1 μg RNA using PrimeScript RT Master Mix (TaKaRa). RT-PCR was performed to measure *Ppp3r2* expression in tissues using ExTaq PCR Master Mix (TaKaRa) in accordance with the manufacturer's protocol. An ABI ProFlex PCR thermal cycler (Applied Biosystems) was used to perform the assay. The sequences of the primers were as follows: *Ppp3r2* (amplification product 723 bp), forward 5′-CCAAACTGAGCTGTGCAACC-3′, reverse 5′-GTTCTTTGTGCCCCGAGAGA-3′; *β-actin* (amplification product 198 bp), forward 5′-TGAGCTGCGTTTTACACCCT-3′, reverse 5′-GCCTTCACCGTTCCAGTTTT-3′.

Western blot analysis

Testes were homogenized in RIPA lysis buffer (Thermo Fisher Scientific) containing protease inhibitor cocktail (Roche) on ice for 30 min. Sperm were lysed in lysis buffer (6 M urea, 2 M thiourea, and 2% sodium deoxycholate) for 15 min at room temperature. Then the lysates were centrifuged at 15000 *g* for 10 min. The proteins in the supernatant were collected, and

the protein concentrations were determined with a BCA protein assay kit (Thermo Fisher Scientific).

Protein samples (20 μg) were separated using 8%–16% denaturing polyacrylamide gels and then transferred to polyvinylidene difluoride membranes (Millipore). Membranes were blocked with 5% bovine serum albumin (BSA) for 1 h at room temperature, and immunoblotting was performed overnight at 4°C with the primary antibodies against PPP3R2 (1:2000 dilution, Abcam), ABCA1 (1:2000 dilution, Abcam), and β-actin (1:5000 dilution, Abcam), followed by incubation with secondary antibody conjugated to HRP (Jackson ImmunoResearch). Signals were generated by enhanced chemiluminescence (Millipore) and detected with a luminescent image analyzer (GE Imagination LAS 4000).

Immunofluorescence analysis

Immunofluorescence staining was performed using standard protocols. Frozen testicular sections (8-μm thick) or sperm smears were prepared and then fixed with 4% paraformaldehyde for 20 min at 4°C. The unspecific binding sites were blocked with 10% BSA/PBS for 60 min at room temperature, and then sections were incubated with the primary antibodies against PPP3R2 (1:200 dilution, Abcam), α-tubulin (1:400 dilution, Abcam), Basigin (1:400 dilution, Abcam), septin 4 (1:200 dilution, Abcam), ABCA1 (1:400 dilution, Abcam), and caveolin-1 (1:200 dilution, Abcam) overnight at 4°C. Then fluorescent-labeled secondary antibodies (1:500, donkey anti-mouse Alexa Fluor 488 or donkey anti-rabbit Alexa Fluor 555, Jackson ImmunoResearch) were used. Nuclei were counterstained with DAPI (Sigma-Aldrich). The fluorescence signals were detected under a laser scanning confocal microscope (Carl Zeiss LSM-510). Digital images were captured and processed using the Aim software (Zeiss Systems).

Fertility evaluation

Individually housed, sexually mature male mice (10 weeks old) cohabitated with two virgin female mice (10 weeks old). The females were checked for the presence of vaginal plugs as evidence of mating. Approximately, 20 days after the last day of cohabitation, the number of pups delivered by each mated female mouse was counted and the litter sizes were calculated.

Sperm parameter analysis

The cauda epididymides were dissected and then placed in pre-warmed (37°C) Tyrode's buffer (Sigma-Aldrich) to allow dispersion of sperm. After 15 min, sperm suspensions were collected and sperm motility, progressive motility, and concentration were analyzed by CASA (Hamilton Thorne). Moreover, in sperm motility rescue assays, sperm suspensions were incubated with 10 μM db-cAMP (Sigma-Aldrich) or 0.5 μM calcium ionophore A23187 (Sigma-Aldrich) for 15 or 30 min, and then sperm motility was analyzed by CASA.

For teratozoospermia analysis, the sperm pellet was initially smeared on a glass slide. After reaching dryness at room temperature, the slide was fixed and stained as described in the Diff-Quick method (BRED Life Science Technology Inc.). The slide was viewed under a microscope (Olympus BX53). On the other hand, for electron microscopy analysis, the sperm pellet was fixed overnight in 2.5% glutaraldehyde buffer.

For sperm acrosome reaction analysis, sperm suspensions were incubated with 5 μM calcium ionophore A23187 for 30 min, and then FITC–peanut agglutinin (PNA) (Sigma-Aldrich) was applied to identify sperm acrosomal status and detected with laser scanning confocal microscope. The percentage of acrosome-reacted sperm was calculated by evaluating at least 300 sperm per test.

Histological analysis

Testes and epididymides fixed in Bouin's solution were embedded in paraffin, and specimens were sliced into 5-mm-thick sections and mounted on glass slides, followed by deparaffinization and rehydration. The sectioned testicular and epididymal tissues were then stained with H&E and observed under a microscope (Olympus BX53).

Transmission electron microscopy analysis

Small pieces of testicular tissue or sperm precipitate were immersed in 2.5% glutaraldehyde solubilized in 0.1 M phosphate buffer (pH 7.4) for one day. The tissues were then fixed in 1% osmium tetroxide and dehydrated through a graded ethanol series and embedded in Epon 618 (TAAB Laboratories Equipment). Ultrathin sections (70–90 nm) in the seminiferous epithelium region were stained with lead citrate and uranyl acetate and then examined at 100 kV with a Philips CM-120 microscope (Philips).

Sperm cAMP, Ca^{2+}, cholesterol, and capacitation measurements

Mature sperm collected from the caudal epididymis in a Percoll gradient were diluted to 1×10^7/ml. Then, sperm cholesterol was stained with the Amplex Red cholesterol assay (Molecular Probe), and sperm cAMP was detected with a cAMP assay kit (Abcam), according to the manufacturer's instructions.

Meanwhile, sperm suspensions from the caudal epididymis (nearly 5×10^6/ml) were incubated with Fluo-4, acetoxymethyl ester (5 μM, Dojindo) (Liu et al., 2012), filipin (100 μg/ml, Sigma) (Takeo et al., 2008), or M540 (2.6 μM, Sigma) (Martin et al., 2005) for 30 min. After washing with PBS, the fluorescence signals of Fluo-4 for calcium, filipin for membrane cholesterol, and M540 for membrane fluidity were detected using flow cytometry (Becton Dickinson, Beckman Coulter). The CellQuest software analyzed the emission originating from at least 30000 events (Beckman Coulter), and three experiments were repeated for each sperm sample.

Serum analysis and inflammatory cytokine analyses by ELISA

Gonadal hormones such as testosterone (R&D Systems), estradiol (Cayman Chemical), and anti-sperm antibody (MLbio)

in mouse serum (at the age of 10 weeks) were detected with immunoassay kits according to the manufacturer's protocols.

Meanwhile, proinflammatory cytokines such as IL-1β, IL-6, and TNF-α in the testis and epididymis were also detected with immunoassay kits (Ray Biotech) according to the manufacturer's protocols.

CsA administration

To provide additional evidence confirming the function of sperm calcineurin in supporting sperm quality, CsA, a calcineurin inhibitor, was applied to treat WT mice (6 weeks old) *in vivo*, as previously described (Miyata et al., 2015). CsA (Sigma-Aldrich) dissolved in ethanol (200 mg/ml) was diluted in Cremophor EL (Sigma-Aldrich) at a final concentration of 10 mg/ml. The diluted reagent (200 µl; 5 mg CsA/kg bodyweight) was administered to male mice every day by subcutaneous injection. Ethanol diluted in Cremophor EL was used as a control. After 15 days of treatment, cauda sperm were isolated and their parameters and protein expression patterns were characterized.

Statistical analysis

All data were analyzed using the SAS 8.2 software, and results are presented as mean ± SD. Group comparisons were made using Student's *t*-test where appropriate. One-way analysis of variance test was used assuming a two-tailed hypothesis with $P < 0.05$. The comparison of acrosome reaction rate and sperm deformity was assessed by chi-square analysis. Differences were considered statistically different when $P < 0.05$.

Supplementary material

Supplementary material is available at *Journal of Molecular Cell Biology* online.

Acknowledgements

We appreciate the support from Prof. Minghan Tong (Shanghai Institute of Biochemistry and Cell Biology, Chinese Academy of Sciences) for providing *Ppp3r2* KO mice. The authors also thank Ms Rong Fu (Core Facility of Basic Medical Sciences, Shanghai Jiao Tong University School of Medicine) for her technical assistance in flow cytometry assay. The authors are grateful to Prof. Peter Reinach (State University of New York) for his enthusiastic involvement in helping write the more understandable and accurate text.

Funding

This research project was supported by grants from the National Natural Science Foundation of China (81571487, 81701503, and 81971437) and Science and Technology Commission of Shanghai Municipality (16ZR1418600).

Conflict of interest: none declared.

Author contributions: Y.L. conducted and performed experiments, analyzed data, and prepared the manuscript. C.Z. and S.W. performed part of molecular experiments and analyzed some data. Y.H. performed histological analysis and part of molecular experiments. J.J. performed part of sperm motility analysis. L.Y. and R.J. performed part of molecular experiments. Z.D. designed and supervised the project and revised and provided final approval of the manuscript.

References

Aitken, R.J., and Nixon, B. (2013). Sperm capacitation: a distant landscape glimpsed but unexplored. Mol. Hum. Reprod. *19*, 785–793.

Bickel, P.E., Scherer, P.E., Schnitzer, J.E., et al. (1997). Flotillin and epidermal surface antigen define a new family of caveolae-associated integral integral membrane proteins. J. Biol. Chem. *272*, 13793–13802.

Bou Khalil, M., Chakrabandhu, K., Xu, H., et al. (2006). Sperm capacitation induces an increase in lipid rafts having zona pellucida binding ability and containing sulfogalactosylglycerolipid. Dev. Biol. *290*, 220–235.

Chakrabarti, R., Kline, D., Lu, J., et al. (2007). Analysis of Ppp1cc-null mice suggests a role for PP1γ2 in sperm morphogenesis. Biol. Reprod. *76*, 992–1001.

Christova, Y., James, P., Mackie, A., et al. (2004). Molecular diffusion in sperm plasma membranes during epididymal maturation. Mol. Cell. Endocrinol. *216*, 41–46.

Cross, N.L. (2004). Reorganization of lipid rafts during capacitation of human sperm. Biol. Reprod. *71*, 1367–1373.

Dacheux, J.L., and Dacheux, F. (2013). New insights into epididymal function in relation to sperm maturation. Reproduction *147*, 27–42.

De Jonge, C. (2017). Biological basis for human capacitation-revisited. Hum. Reprod. Update *23*, 289–299.

Dell'Acqua, M.L., Smith, K.E., Gorski, J.A., et al. (2006). Regulation of neuronal PKA signaling through AKAP targeting dynamics. Eur. J. Cell Biol. *85*, 627–633.

Dittmer, P.J., Dell'Acqua, M.L., and Sather, W.A. (2014). Ca^{2+}/calcineurin-dependent inactivation of neuronal L-type Ca^{2+} channels requires priming by AKAP-anchored protein kinase A. Cell Rep. *7*, 1410–1416.

Dun, M.D., Aitken, R.J., and Nixon, B. (2012). The role of molecular chaperones in spermatogenesis and the post-testicular maturation of mammalian spermatozoa. Hum. Reprod. Update *18*, 20–35.

Forgione, N., Vogl, A.W., and Varmuza, S. (2010). Loss of protein phosphatase 1cγ (PPP1CC) leads to impaired spermatogenesis associated with defects in chromatin condensation and acrosome development: an ultrastructural analysis. Reproduction *139*, 1021–1029.

Foster, L.J., De Hoog, C.L., and Mann, M. (2003). Unbiased quantitative proteomics of lipid rafts reveals high specificity for signaling factors. Proc. Natl Acad. Sci. USA *100*, 5813–5818.

Freitas, M.J., Vijayaraghavan, S., and Fardilha, M. (2017). Signaling mechanisms in mammalian sperm motility. Biol. Reprod. *96*, 2–12.

Gadella, B.M., and Boerke, A. (2016). An update on post-ejaculatory remodeling of the sperm surface before mammalian fertilization. Theriogenology *85*, 113–124.

Gervasi, M.G., and Visconti, P.E. (2017). Molecular changes and signaling events occurring in spermatozoa during epididymal maturation. Andrology *5*, 204–218.

Gillan, L., Evans, G., and Maxwell, W.M. (2005). Flow cytometric evaluation of sperm parameters in relation to fertility potential. Theriogenology *63*, 445–457.

Goswami, S., Korrodi-Gregório, L., Sinha, N., et al. (2019). Regulators of the protein phosphatase PP1γ2, PPP1R2, PPP1R7, and PPP1R11 are involved in epididymal sperm maturation. J. Cell. Physiol. *234*, 3105–3118.

Haidar, B., Denis, M., Krimbou, L., et al. (2002). cAMP induces ABCA1 phosphorylation activity and promotes cholesterol efflux from fibroblasts. J. Lipid Res. *43*, 2087–2094.

Haidar, B., Denis, M., Marcil, M., et al. (2004). Apolipoprotein A-I activates cellular cAMP signaling through the ABCA1 transporter. J. Biol. Chem. *279*, 9963–9969.

Hu, Y.W., Ma, X., Li, X.X., et al. (2009). Eicosapentaenoic acid reduces ABCA1 serine phosphorylation and impairs ABCA1-dependent cholesterol efflux through cyclic AMP/protein kinase A signaling pathway in THP-1 macrophage-derived foam cells. Atherosclerosis *204*, e35–e43.

Huang, Z., and Vijayaraghavan, S. (2004). Increased phosphorylation of a distinct subcellular pool of protein phosphatase, PP1γ2, during epididymal sperm maturation. Biol. Reprod. *70*, 439–447.

Ihara, M., Kinoshita, A., Yamada, S., et al. (2005). Cortical organization by the septin cytoskeleton is essential for structural and mechanical integrity of mammalian spermatozoa. Dev. Cell *8*, 343–352.

Karwatsky, J., Ma, L., Dong, F., et al. (2010). Cholesterol efflux to apoA-I in ABCA1-expressing cells is regulated by Ca^{2+}-dependent calcineurin signaling. J. Lipid Res. *51*, 1144–1156.

Kissel, H., Georgescu, M.M., Larisch, S., et al. (2005). The Sept4 septin locus is required for sperm terminal differentiation in mice. Dev. Cell *8*, 353–364.

Klee, C.B., Ren, H., and Wang, X. (1998). Regulation of the calmodulin-stimulated protein phosphatase, calcineurin. J. Biol. Chem. *273*, 13367–13370.

Koch, S., Acebron, S.P., Herbst, J., et al. (2015). Post-transcriptional Wnt signaling governs epididymal sperm maturation. Cell *163*, 1225–1236.

Kuo, Y.C., Lin, Y.H., Chen, H.I., et al. (2012). SEPT12 mutations cause male infertility with defective sperm annulus. Hum. Mutat. *33*, 710–719.

Kuo, Y.C., Shen, Y.R., Chen, H.I., et al. (2015). SEPT12 orchestrates the formation of mammalian sperm annulus by organizing core octameric complexes with other SEPT proteins. J. Cell Sci. *128*, 923–934.

Lawn, R.M., Wade, D.P., Garvin, M.R., et al. (1999). The Tangier disease gene product ABC1 controls the cellular apolipoprotein-mediated lipid removal pathway. J. Clin. Invest. *104*, R25–R31.

Le Goff, W., Peng, D.Q., Settle, M., et al. (2004). Cyclosporin A traps ABCA1 at the plasma membrane and inhibits ABCA1-mediated lipid efflux to apolipoprotein A-I. Arterioscler. Thromb. Vasc. Biol. *24*, 2155–2161.

Leahy, T., and Gadella, B.M. (2015). New insights into the regulation of cholesterol efflux from the sperm membrane. Asian J. Androl. *17*, 561–567.

Lester, L.B., Faux, M.C., Nauert, J.B., et al. (2001). Targeted protein kinase A and PP-2B regulate insulin secretion through reversible phosphorylation. Endocrinology *142*, 1218–1227.

Lin, C.H., Shen, Y.R., Wang, H.Y., et al. (2019). Regulation of septin phosphorylation: SEPT12 phosphorylation in sperm septin assembly. Cytoskeleton *76*, 137–142.

Lin, Y.H., Kuo, Y.C., Chiang, H.S., et al. (2011). The role of the septin family in spermiogenesis. Spermatogenesis *1*, 298–302.

Liu, Y., Qu, F., Cao, X., et al. (2012). Con A-binding protein Zn-α2-glycoprotein on human sperm membrane is related to acrosome reaction and sperm fertility. Int. J. Androl. *35*, 145–157.

Martin, G., Sabido, O., Durand, P., et al. (2005). Phosphatidylserine externalization in human sperm induced by calcium ionophore A23187: relationship with apoptosis, membrane scrambling and the acrosome reaction. Hum. Reprod. *20*, 3459–3468.

Martin-DeLeon, P.A. (2015). Epididymosomes: transfer of fertility-modulating proteins to the sperm surface. Asian J. Androl. *17*, 720–725.

Mishra, S., Somanath, P.R., Huang, Z., et al. (2003). Binding and inactivation of the germ cell-specific protein phosphatase PP1γ2 by sds22 during epididymal sperm maturation. Biol. Reprod. *69*, 1572–1579.

Miyata, H., Satouh, Y., Mashiko, D., et al. (2015). Sperm calcineurin inhibition prevents mouse fertility with implications for male contraceptive. Science *350*, 442–445.

Morales, C.R., Marat, A.L., Ni, X., et al. (2008). ATP-binding cassette transporters ABCA1, ABCA7, and ABCG1 in mouse spermatozoa. Biochem. Biophys. Res. Commun. *376*, 472–477.

Nagao, K., Maeda, M., Mañucat, N.B., et al. (2013). Cyclosporine A and PSC833 inhibit ABCA1 function via direct binding. Biochim. Biophys. Acta *1831*, 398–406.

Nishiuchi, Y., Murao, K., Imachi, H., et al. (2010). Transcriptional factor prolactin regulatory element-binding protein-mediated gene transcription of ABCA1 via 3′,5′-cyclic adenosine-5′-monophosphate. Atherosclerosis *212*, 418–425.

Oram, J.F., Lawn, R.M., Garvin, M.R., et al. (2000). ABCA1 is the cAMP-inducible apolipoprotein receptor that mediates cholesterol secretion from macrophages. J. Biol. Chem. *275*, 34508–34511.

Ouvrier, A., Cadet, R., Vernet, P., et al. (2009). LXR and ABCA1 control cholesterol homeostasis in the proximal mouse epididymis in a cell-specific manner. J. Lipid Res. *50*, 1766–1775.

Palme, N., Becher, A.C., Merkl, M., et al. (2014). Immunolocalization of the cholesterol transporters ABCA1 and ABCG1 in canine reproductive tract tissues and spermatozoa. Reprod. Domest. Anim. *49*, 441–447.

Pan, X., Chen, X., Tong, X., et al. (2015). Ppp2ca knockout in mice spermatogenesis. Reproduction *149*, 385–391.

Puga Molina, L.C., Luque, G.M., Balestrini, P.A., et al. (2018). Molecular basis of human sperm capacitation. Front. Cell Dev. Biol. *6*, 72.

Rejraji, H., Sion, B., Prensier, G., et al. (2006). Lipid remodeling of murine epididymosomes and spermatozoa during epididymal maturation. Biol. Reprod. *74*, 1104–1113.

Rusnak, F., and Mertz, P. (2000). Calcineurin: form and function. Physiol. Rev. *80*, 1483–1521.

Saez, F., Ouvrier, A., and Drevet, J.R. (2011). Epididymis cholesterol homeostasis and sperm fertilizing ability. Asian J. Androl. *13*, 11–17.

Selva, D.M., Hirsch-Reinshagen, V., Burgess, B., et al. (2004). The ATP-binding cassette transporter 1 mediates lipid efflux from Sertoli cells and influences male fertility. J. Lipid Res. *45*, 1040–1050.

Shen, Y.R., Wang, H.Y., Kuo, Y.C., et al. (2017). SEPT12 phosphorylation results in loss of the septin ring/sperm annulus, defective sperm motility and poor male fertility. PLoS Genet. *13*, e1006631.

Silva, J.V., Freitas, M.J., and Fardilha, M. (2014). Phosphoprotein phosphatase 1 complexes in spermatogenesis. Curr. Mol. Pharmacol. *7*, 136–146.

Simons, K., and Toomre, D. (2000). Lipid rafts and signal transduction. Nat. Rev. Mol. Cell Biol. *1*, 31–39.

Sinha, N., Puri, P., Nairn, A.C., et al. (2013). Selective ablation of Ppp1cc gene in testicular germ cells causes oligo-teratozoospermia and infertility in mice. Biol. Reprod. *89*, 128.

Smart, E.J., Graf, G.A., McNiven, M.A., et al. (1999). Caveolins, liquid-ordered domains, and signal transduction. Mol. Cell. Biol. *19*, 7289–7304.

Takeo, T., Hoshii, T., Kondo, Y., et al. (2008). Methyl-β-cyclodextrin improves fertilizing ability of C57BL/6 mouse sperm after freezing and thawing by facilitating cholesterol efflux from the cells. Biol. Reprod. *78*, 546–551.

Thaler, C.D., Thomas, M., and Ramalie, J.R. (2006). Reorganization of mouse sperm lipid rafts by capacitation. Mol. Reprod. Dev. *73*, 1541–1549.

Travis, A.J., and Kopf, G.S. (2002). The role of cholesterol efflux in regulating the fertilization potential of mammalian spermatozoa. J. Clin. Invest. *110*, 731–736.

Vadnais, M.L., Aghajanian, H.K., Lin, A., et al. (2013). Signaling in sperm: toward a molecular understanding of the acquisition of sperm motility in the mouse epididymis. Biol. Reprod. *89*, 127.

Vijayaraghavan, S., Chakrabarti, R., and Myers, K. (2007). Regulation of sperm function by protein phosphatase PP1γ2. Soc. Reprod. Fertil. Suppl. *63*, 111–121.

Vijayaraghavan, S., Stephens, D.T., Trautman, K., et al. (1996). Sperm motility development in the epididymis is associated with decreased glycogen synthase kinase-3 and protein phosphatase 1 activity. Biol. Reprod. *54*, 709–718.

Voss, M., Fechner, L., Walz, B., et al. (2010). Calcineurin activity augments cAMP/PKA-dependent activation of V-ATPase in blowfly salivary glands. Am. J. Physiol. Cell Physiol. *298*, C1047–C1056.

Watanabe, H., and Kondoh, G. (2011). Mouse sperm undergo GPI-anchored protein release associated with lipid raft reorganization and acrosome reaction to acquire fertility. J. Cell Sci *124*, 2573–2581.

Whitfield, M., Pollet-Villard, X., Levy, R., et al. (2015). Posttesticular sperm maturation, infertility, and hypercholesterolemia. Asian J. Androl. *17*, 742–748.